Density-functional theory calculations of the adsorption of Cl at perfect and defective Ag(111) surfaces

N. H. de Leeuw,[1,2,*] C. J. Nelson,[2,3] C. R. A. Catlow,[1,3] P. Sautet,[4] and W. Dong[4]
[1]*Department of Chemistry, University College, University of London, 20 Gordon Street, London WC1H 0AJ, United Kingdom*
[2]*School of Crystallography, Birkbeck College, University of London, Malet Street, London WC1E 7HX, United Kingdom*
[3]*Davy Faraday Research Laboratory, Royal Institution of Great Britain, Albemarle Street, London W1X 4BS, United Kingdom*
[4]*Laboratoire de Chimie, UMR CNRS 5182, Ecole Normale Supérieure de Lyon, 46 Allé d'Italie, 69364 Lyon Cedex 07, France*

(Received 16 July 2003; revised manuscript received 9 October 2003; published 28 January 2004)

Density functional theory calculations of adsorption of chlorine at the perfect and defective silver (111) surface have shown that the energies of adsorption of chlorine atoms show little variation (less than 30 kJ mol^{-1}) between the different sites, from -136 kJ mol^{-1} next to a silver adatom, through -159 kJ mol^{-1} at the perfect surface to -166 kJ mol^{-1} next to a silver vacancy at the surface. Molecular chlorine adsorbs in a series of energetically similar overlayers, which are in good agreement with experimentally found structures. The lowest energy configuration is a planar hexagonal honeycomb structure of chlorine atoms adsorbed in fcc and hcp hollow sites on the silver surface. An energetically similar structure is geometrically nonplanar, but has a planar electronic structure. Although the chlorine molecules are virtually dissociated (Cl-Cl distance$=3.40$ Å), significant electron density is distributed along the Cl-Cl axes, leading to a network of electronic interactions between the adsorbed chlorine atoms. The adsorption energy for Cl_2 is calculated at -231 kJ mol^{-1}, in good agreement with experiment. Calculated Ag-Cl bond lengths of 2.69, 2.47, and 2.33 Å agree with several experimental studies and show that the different bond lengths found experimentally are not anomalous, but due to the formation of geometrically different but energetically almost identical chlorine overlayer structures.

DOI: 10.1103/PhysRevB.69.045419 PACS number(s): 68.03.−g, 68.43.Fg, 68.43.Bc, 68.47.De

INTRODUCTION

Silver is of considerable industrial importance as a catalytic material, particularly in the selective partial oxidation of ethene to its epoxide, which is a widely used precursor for many chemical products.[1,2] As a consequence of its catalytic significance and also because of the ease with which silver is investigated using surface science techniques, such as scanning tunnelling microscopy (STM) by, for example, Refs. 3 and 4, silver surfaces have been the subject of much research, both experimentally,[5–8] and theoretically.[9–14] Often, the reactivity of the metal is probed by the adsorption of small molecules, for example NO,[15,16] CO_2,[17] or SiO and SiS,[18] while a variety of experimental techniques has been used to study the interactions of silver with a host of small organic adsorbates, such as methanol,[19] phenol,[20] t-butyl nitrite[21] and sulfur-containing compounds.[22–24] More recently, experimental techniques have been employed to study the synthesis and behavior of silver nanoparticles; see, e.g., Refs. 25 and 26.

As oxygen plays a crucial rôle in the catalytic epoxidation process,[27,28] its presence and behavior at the silver surface has been studied by a number of groups, often as the main species under investigation, for example the STM study by Carlisle *et al.* of the formation of an oxide film at the silver (111) surface,[29] the effects of oxygen on silver morphology,[30,31] or the theoretical studies of oxygen adsorption by Li *et al.*[32] and Wang *et al.*,[33] oxygen dissociation on Ag(110) surfaces by Salazar *et al.*,[34] and combined experimental and theoretical studies of silver oxide phases on the Ag(111) surface.[35,36] Oxygen as a coadsorbate has also been studied extensively by a variety of techniques, e.g., the spectroscopic study of ethene and ethene oxide adsorption on an oxygen-covered Ag(111) surface by Stacchiola *et al.*[37] and the computational studies by Avdeev and Zhidomirov[38] and Sun *et al.*[39] of the adsorption of ethene and methanol, respectively, on oxidized silver surfaces. More recently, Bocquet *et al.* have used a combination of density functional theory calculations and STM experiments to investigate ethene epoxidation on the silver (111) surface.[40,41]

The bare silver metal, however, is often not very selective in catalytic partial oxidation processes; but after exposure to and subsequent adsorption of chlorine the metal is observed to demonstrate a significantly increased selectivity towards the desired reaction product; see, for instance, Ref. 42. As a result, the interaction of halogens or halide-containing adsorbates with silver surfaces has been widely studied experimentally, for example by the use of scanning tunnelling microscopy,[43] temperature-programmed desorption[44] and a range of spectroscopic techniques.[45,46] However, computational studies have often concentrated on the ideal surfaces[47–49] whereas real surfaces contain significant numbers of defects. In this work we have therefore employed electronic structure calculations based on density functional theory (DFT) to investigate the adsorption of chlorine not only at the perfect (111) surface of silver metal, but also at three defective silver (111) surfaces; one surface consisting of a series of (111) terraces offset from each other by monatomic steps, and two (111) planes which are partially vacant in silver atoms. Our studies reveal that the energies of adsorption of chlorine atoms show little variation between dif-

ferent surface sites and that molecular chlorine adsorbs in a series of energetically similar overlayers, which are in good agreement with experimentally found structures.

THEORETICAL METHODS

The total energy and structure of the silver surfaces were calculated using the plane-wave pseudo-potential techniques available in the Vienna *ab initio* Simulation Program (VASP).[50–53] The basic concepts of DFT and the principles of applying DFT to pseudopotential plane-wave calculations have been extensively reviewed elsewhere, for example, in Refs. 54–56. Furthermore, this methodology is well established and has been successfully applied to the study of metals,[57,58] semiconductors,[59,60] and ionic materials.[61–63] The calculations were performed within the generalized-gradient approximation, using the exchange-correlation potential developed by Perdew *et al.*,[64] which approach has been shown to give reliable results for a range of metals and ionic materials, shown, for example, in Refs. 65–67. Within the pseudopotential approach only the valence electrons are treated explicitly and the pseudopotential represents the effective interaction of the valence electrons with the atomic cores. The valence orbitals are represented by a plane wave basis set, in which the energy of the plane-waves is less than a given cutoff (E_{cut}), where the magnitude of E_{cut} required to converge the total energy of the system has important implications for the size of the calculation. The VASP program employs ultrasoft pseudopotentials,[68,69] which allows the use of a smaller basis set for a given accuracy. In our calculations the core consisted of orbitals up to and including the $3d$ orbital for Ag, leaving the $4d$ and $5s$ electrons to be treated explicitly, and up to and including the $2p$ orbital for Cl.

For surface calculations, where two energies are compared, it is important that the total energies are well converged. The degree of convergence depends on a number of factors, two of which are the plane-wave cutoff and the density of k-point sampling within the Brillouin zone. We have investigated these by undertaking a number of calculations for bulk silver with different values for these parameters. We have, by means of these test calculations, determined values for E_{cut} (300 eV) and the size of the Monkhorst-Pack k-point mesh[70] ($11\times11\times11$) so that the total energy is converged to within $0.03\,\mathrm{kJ\,mol^{-1}}$ ($<0.01\%$). The optimization of the atomic coordinates (and unit cell size/shape for the bulk material) was performed via a conjugate gradients technique which utilizes the total energy and the Hellmann-Feynman forces on the atoms (and stresses on the unit cell). We used the common approach for modelling the surfaces, using three-dimensional periodic boundary conditions by considering slabs of Ag. Therefore, in addition to the k-point density and E_{cut} discussed above, the convergence in surface calculations also depends on the thickness of the slab of material and the width of the vacuum layer between the slabs. Again, we checked convergence by running a series of test calculations with different slab thicknesses and gap widths, which showed that a slab thickness of five silver layers was sufficient for the energy to converge and on the basis of these test calculations, we ensured that in each calculation the vacuum layer was at least 16 Å between the images of the surfaces either side of the void. The Methfessel-Paxton method[71] with a smearing width of 0.20 eV was chosen to determine how the partial occupancies are set for each wave function, which method gives an accurate description of the total energy of the system.

RESULTS

Silver has a face-centered-cubic structure. The experimental lattice parameters of silver are $a=b=c=4.101$ Å,[72] which upon full electronic and geometry optimization expanded slightly to 4.161 Å, i.e., an error of $\sim1.5\%$. The (111) surface, which is a hexagonal close-packed plane of silver atoms, is the most stable[73] and we thus concentrate on this surface in this study of the adsorption of chlorine. As experimental surfaces are never perfect and catalytic processes often occur at surface defects, such as vacancies, steps, and growth islands, we have investigated chlorine adsorption at different surface features, i.e. on the terrace of the perfect surface; in or next to a surface vacancy; at a surface adatom; and on or below a monatomic step on the (111) surface. Previous work has shown that these surface defects, shown in Fig. 1, have low formation energies compared to the perfect surface and, therefore, that these surface features can be expected to occur on experimental (111) surfaces.[65] The perfect surface shows very little atomic relaxation of the surface atoms with respect to the bulk metal, in line with experiment,[74] although the electron density is more delocalised along the surface compared to the bulk. On the defective surfaces, the electron density is distributed in such a way as to minimize the effect of the defect, e.g., smoothing the step and adatom edges and filling the vacancy, through a more gradual decline of electron density in the defect areas than is observed at the perfect surface. Atomic relaxation of the surface areas surrounding the defects also plays a role in stabilizing the defective surface, especially shortening the Ag-Ag bonds in the immediate defect region.

We first investigated the adsorption of chlorine atoms at the different surface sites to determine the most stable adsorption sites and adsorption energies, before considering the adsorption of a chlorine molecule. As chlorine in the gas phase exists as a diatomic molecule, we have calculated the adsorption energy, E_{ads}, according to Eq. (1):

$$E_{\mathrm{ads}}=\frac{E_{\mathrm{slab+Cl}}-[E_{\mathrm{slab}}+1/2nE(\mathrm{Cl_2})]}{n} \tag{1}$$

where $E_{\mathrm{slab+Cl}}$ is the energy of the geometry optimized slab of silver with adsorbed chlorine (per Cl atom), E_{slab} is the energy of the slab of material without adsorbed chlorine, $E(\mathrm{Cl_2})$ is the energy of an isolated $\mathrm{Cl_2}$ molecule and n is the number of adsorbed Cl atoms, all calculated with the same simulation parameters and in equivalent simulation cells to achieve cancellation of basis set errors.[75] The adsorption energy calculated according to Eq. (1) thus takes into account the energy necessary to dissociate the $\mathrm{Cl_2}$ molecule into two Cl atoms, when we explicitly consider adsorption of atomic

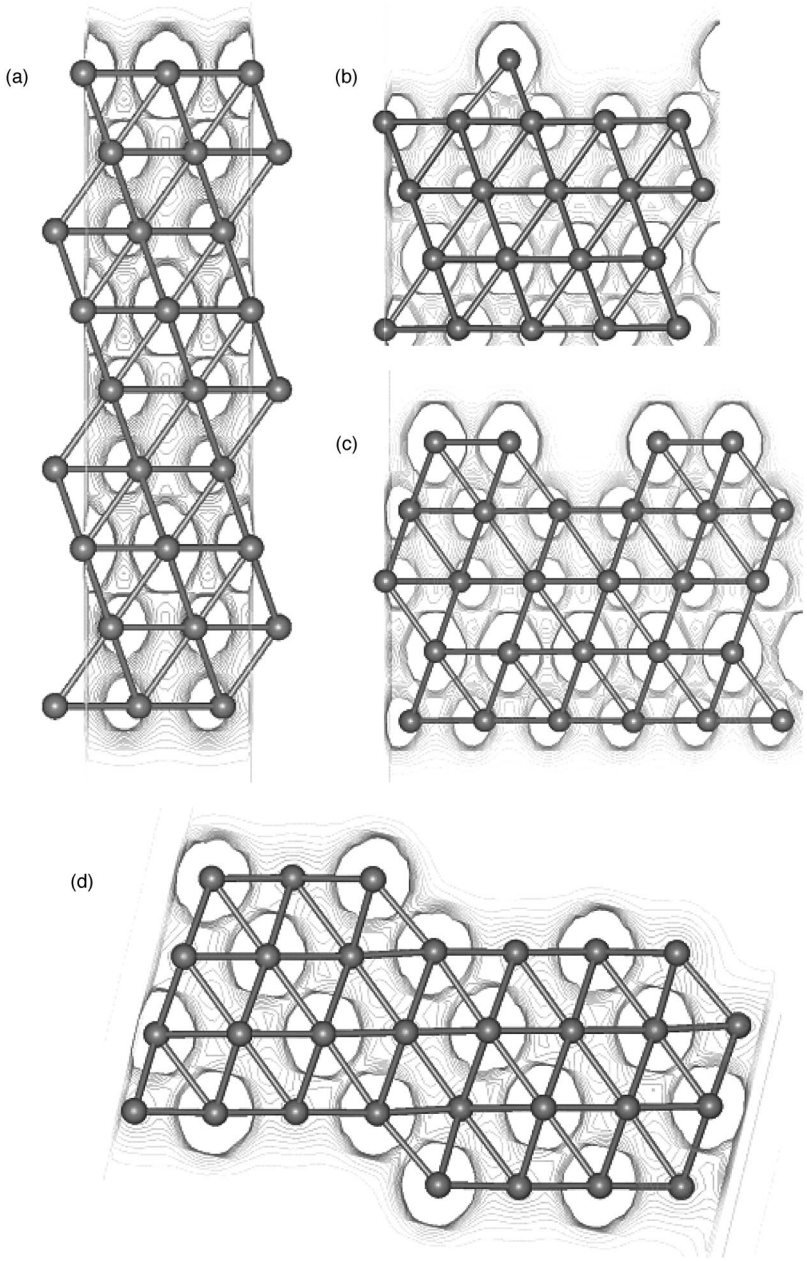

FIG. 1. Side view of geometry optimized structures of (a) the silver slab with (111) surfaces at either end, showing electron density contour plots through the silver atoms of the first, fourth, and seventh layers from the top. (b) The (111) surface covered by 11% adatoms, showing electron density contour plots through the silver adatoms. (c) A slice containing the vacancy of the 11% vacant (111) surface, showing electron density contour plots through the silver vacancy. (d) The stepped (111) surface, showing electron density contour plots through silver atoms on the step edge (electron density contour levels are from $0.02e/Å^3$ to $0.30e/Å^3$ at $0.02e/Å^3$ intervals. The apparent shift of electron density away from the atoms in the other layers is due to the fact that the electron density plane shown is not centred upon those atoms and hence shows electron density in a plane away from the atomic centers).

chlorine. When we investigated adsorption of molecular Cl_2 at the surface, the molecule was left to dissociate during geometry optimization, although a sufficient number of starting configurations of the Cl_2 molecule at the surface was calculated to allow us to be confident that the lowest energy structure had been obtained rather than a local minimum.

Perfect (111) surface

We initially adsorbed chlorine atoms on both sides of a slab of silver material containing the perfect (111) surfaces on both sides, as shown in Fig. 1(a). The stacking of the planes of silver atoms in the (111) direction is *abc*, where the silver atoms in the fourth layer are directly underneath those in the first layer, etc. As a result there are two types of hollow site, each threefold coordinated by three close-packed silver atoms in the surface. One site is on top of a silver atom in the second layer (the hexagonal close packed hcp site), whereas the other hollow site (the face-centered-cubic fcc site) is directly above a silver atom in the third layer. In addition to these hcp and fcc hollow sites, we investigated two other sites for chlorine atom adsorption, i.e., on top of one of the surface silver atoms (top) and on the bridge between an fcc and hcp site (bridge).

In all calculations, the simulation cell consisted of a $\sqrt{3} \times \sqrt{3}R30^0$ supercell, resulting in three silver atoms in each layer, which were then infinitely repeated parallel to the surface by periodic boundary conditions. This modest supercell ensured that the different adsorption sites were separated enough from their images in the mirror cells that the adsorbed chlorine atoms would not interact significantly with each other, and is furthermore capable of simulating the $\sqrt{3} \times \sqrt{3}R30^0$ chlorine coverage found experimentally.[76–78] The entire slab of material, including the chlorine atoms, was

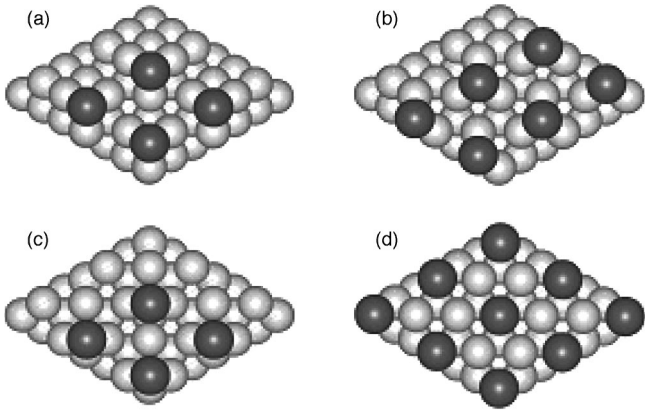

FIG. 2. Plan view of chlorine atoms adsorbed at four different surface sites, i.e., (a) the fcc site, (b) the hcp site, (c) the bridge site, and (d) on top of one of the surface silver atoms (Ag, pale gray; Cl, dark gray).

allowed to relax during the electronic and geometry optimization. However, the chlorine atoms placed on the bridge and top sites moved away upon relaxation towards either a fcc or hcp site, and we therefore kept these chlorine atoms fixed parallel to the plane of the surface, while allowing the distance between slab and chlorine atom to vary normal to the surface. These partially constrained calculations enable us to obtain energies for these unstable adsorption sites, which even if unstable will provide pathways for chlorine atom migration across the surface (see Fig. 2).

The adsorption energies for the different sites are listed in Table I, from which it is clear that the fcc and hcp sites are both equally amenable to Cl adsorption, with a slight energetical preference ($1\,\mathrm{kJ\,mol^{-1}}$) for the fcc site, but that the bridge and especially the top sites are less favourable adsorption sites. However, the difference in adsorption energy between hcp and bridge sites is less than $10\,\mathrm{kJ\,mol^{-1}}$, which although significant is relatively small compared to the large adsorption energies. As such we may expect the initial adsorption of chlorine at the surface to a certain extent to be random between the two hollow sites, with rapid diffusion of adsorbed chlorine atoms away from the top and bridge sites. Adsorption in the two hollow sites, with a preference for the fcc site, is borne out qualitatively by several experimental studies of halogen adsorption at close-packed metal surfaces, for example by Takata *et al.*,[79] who found that chlorine adsorbed preferentially in the fcc sites on the nickel (111) surface. Dhanak *et al.*, on the other hand, also identified the fcc hollow as the preferential site for the adsorption of iodine on the palladium (111) surface,[80] but found that approximately 10% of iodine atoms adsorbed in the hcp sites. Kadodwala *et al.*[81] showed an even larger occupation of 25% of hcp sites on the copper (111) surface by chlorine atoms, in agreement with our calculations which suggest that the hcp site would be an energetically favorable adsorption site as well.

TABLE I. Energies of adsorption of atomic chlorine at different surface sites on the perfect (111) surface.

Adsorption energies of atomic chlorine at the perfect (111) surface (in $\mathrm{kJ\,mol^{-1}}$) and Ag-Cl bond lengths (in Å)

Surface site	Symmetric adsorption at both sides of silver slab	Adsorption at one side of slab only	$r_{Ag\text{-}Cl}$
fcc hollow	−158.1	−156.9	2.66
hcp hollow	−157.2	−156.0	2.66
Bridge	−147.5	−148.2	2.56
Top	−114.9	−109.0	2.40

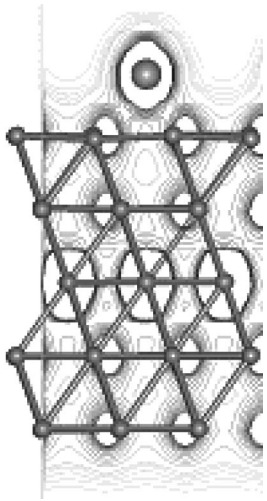

FIG. 3. Side view of the geometry optimized structure of the silver (111) surface with chlorine atom adsorbed at the fcc site, i.e. directly above a silver atom in the third layer, with electron density contour plots through the plane of the chlorine atom (electron density contour levels are from $0.02\mathrm{e/Å^3}$ to $0.30\mathrm{e/Å^3}$ at $0.02\mathrm{e/Å^3}$ intervals).

As the above calculations are computationally expensive, especially once we start calculating adsorption at defective sites, such as vacancies, adatoms and steps, and adsorption of Cl_2, all of which necessitate much larger simulation cells, we investigated whether a different and cheaper procedure would yield similar energies and geometries. We therefore repeated the above calculations for a slab of silver material, where the bottom of five silver layers was kept fixed at its bulk relaxed position, but where the atoms in the other four layers were allowed to move freely during electronic and geometry optimization. Chlorine was only adsorbed at the unrestrained surface, with the necessary dipole correction employed to neutralize the dipole thus created perpendicular to the surface. We once again investigated the adsorption of atomic chlorine at the fcc, hcp and bridge sites and the calculated adsorption energies are also listed in Table I, which shows that the two methods agree to about $1\,\mathrm{kJ\,mol^{-1}}$ in the adsorption energies for the stable adsorption sites, and within $5\,\mathrm{kJ\,mol^{-1}}$ for the unstable adsorption site on top of the silver atom. The relative reactivities of the different sites also show good agreement between the two sites, with the bridge site now less favourable than the fcc site by about $8\,\mathrm{kJ\,mol^{-1}}$. Figure 3 shows the chlorine atom adsorbed at the fcc site, where the electron density contour plots through the plane of the chlorine atom show that up to an electron density distribution of $0.20\mathrm{eÅ^{-3}}$ is distributed along the Ag-Cl bonds, which are partially covalent.

TABLE II. Energies of adsorption of atomic chlorine at surface defects on the (111) surface.

Adsorption energies of atomic chlorine at defect sites on the (111) surface (in kJ mol^{-1})		
Terrace	fcc site	−158.4
Vacancy	In vacancy site	−157.3
	Fcc site next to vacancy	−166.0
Adatom	On adatom	−113.4
	Fcc site next to adatom	−136.3
Step	At step edge	−163.9

On the basis of these calculations of chlorine adsorption at the (111) surface in a $\sqrt{3}\times\sqrt{3}R30^0$ cell, we used the same set up in our subsequent calculations, with a bottom layer of fixed silver atoms and a dipole correction, to obtain the structures and adsorption energies for adsorption at surface defects.

Adsorption at surface defects

For the simulation of chlorine adsorption at surface defects, we needed larger simulation cells to model the various defective surfaces, for example 3×3 supercells for the surfaces with vacancies and adatoms. Clearly, if we are to compare adsorption structures and energies between the different supercells, we need to investigate whether the size of the supercell affects these properties. However, when we investigated whether the use of a larger supercell had any effect on the adsorption energy, we found that the effect was negligible, and that growing the $\sqrt{3}\times\sqrt{3}R30^0$ (111) surface cell to even just a 2×2 supercell was sufficient to avoid the size of the simulation cell or chlorine-chlorine interactions to affect the adsorption energy or adsorbate/substrate structure. The inter-chlorine distances on the $\sqrt{3}\times\sqrt{3}R30^0$ and 2×2 surfaces are 5.1 and 5.9 Å, respectively, which is far more than twice the van der Waals radius of chlorine (3.6 Å), and direct interactions between the adsorbed chlorine atoms are therefore negligible even on the $\sqrt{3}\times\sqrt{3}R30^0$ surface. The difference in adsorption energies in the fcc site between the $\sqrt{3}\times\sqrt{3}R30^0$ and 2×2 surface cells is only 1.5 kJ mol^{-1}, and this small difference in adsorption energies is due to a slightly more extensive relaxation of the surface silver atoms around the adsorbed chlorine atom in the 2×2 cell. Whereas after electronic relaxation only, the energy released upon adsorption of atomic chlorine at the 2×2 surface cell is only 40.9 kJ mol^{-1}, upon full geometry optimization this adsorption energy increases to 158.4 kJ mol^{-1}, clearly showing that atomic relaxation is the major contributory factor to the adsorption energies. The close agreement in structures and energies between the $\sqrt{3}\times\sqrt{3}R30^0$ and 2×2 supercells shows that the size of the simulation supercell does not affect the adsorption energies, which are listed in Table II for the defect sites.

We first studied adsorption of atomic chlorine on a (111) plane, where one of each nine surface atoms had been removed, leaving an 11% concentration of isolated surface vacancies [see Fig. 1(c)]. In addition to a partially vacant surface, we also investigated the effect of isolated silver atoms added to the surface. Again we studied a 3×3 surface supercell, this time with an 11% coverage of isolated silver atoms on the (111) plane [see Fig. 1(b)]. Finally, we studied a stepped (111) surface to investigate how the adsorption behavior is affected by the presence of an extended step edge of low-coordinated surface atoms instead of isolated point defects. Unlike the surface vacancy and adatom calculations above, the steps on the (111) surface were not formed from defects on the 3×3 planar supercell, as this would lead to a surface containing either one missing row of silver atoms or two missing rows (i.e., one row of adatoms), which would not be a realistic model for a stepped surface. The stepped surface was therefore created by adjusting the lattice vectors of the supercell to form a repeating slab, where the repeat unit was offset by one atomic layer with respect to the first cell. As a result the simulation cell has a true step at the surface, which is repeated from cell to cell, with a terrace of three silver atoms deep between the steps [see Fig. 1(d)].[65] This method of creating stepped planes, which has also been successfully employed in previous simulations of stepped calcite and forsterite surfaces,[82] avoids the occurrence of two opposing steps in a single simulation cell, which would lead to a crenellated rather than a truly stepped surface.

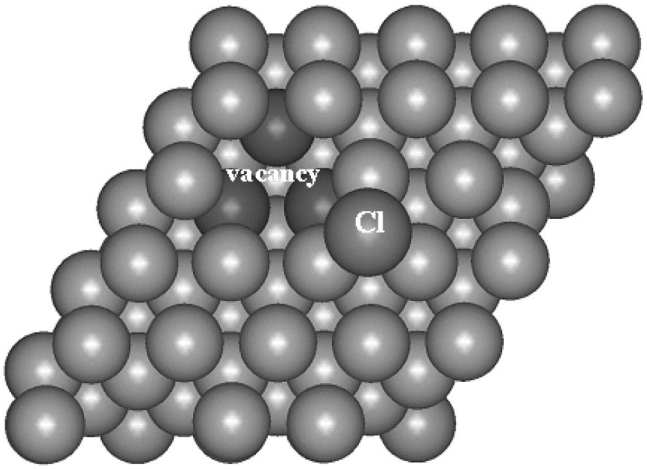

FIG. 4. Plan view of the 11% vacant (111) surface, with chlorine atom adsorbed in a fcc site next to the vacancy, where the silver atoms in the second layer underneath the vacancy are shaded darker (Ag, light gray; Cl, dark gray).

When a vacancy is introduced in the surface, the chlorine atom can either adsorb at the vacancy site or in its vicinity. In addition to the vacancy site itself, we have also calculated the adsorption energy when the chlorine atom becomes adsorbed in an fcc site next to the vacancy. We see, from the energies in Table II. that adsorption in the vacancy site itself releases about the same energy as adsorption at the fcc site of the perfect surface (157.3 versus 158.4 kJ mol^{-1}). However, adsorption in the fcc site next to the vacancy (Fig. 4) has become more favourable compared to the perfect surface, releasing 166.0 kJ mol^{-1}, although the difference in energies is so small (less than 8 kJ mol^{-1}) that in view of the large energies released upon adsorption at the perfect sites, we do not expect it to cause a significant preferential adsorption of

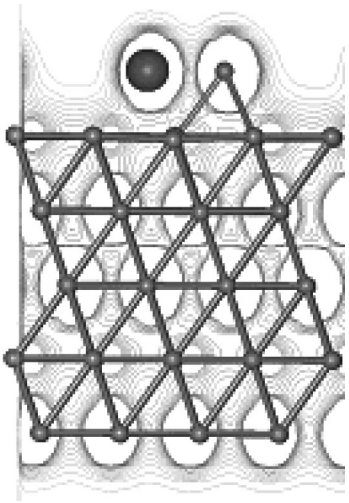

FIG. 5. Side view of chlorine adsorption at the fcc site next to the silver adatom (electron density contour levels are from 0.02 to 0.30e/Å^3 at 0.02e/Å^3 intervals).

chlorine near vacancy sites. The chlorine adsorbed near the vacancy is interacting more strongly with the surface silver atoms than on the perfect surface. Whereas the Ag-Cl bonds to the three surface silver atoms surrounding the fcc site on the perfect surface is 2.66 Å (for both the $\sqrt{3}\times\sqrt{3}R30^0$ and 2×2 surface cells), next to the vacancies the Ag-Cl bonds have shortened to two short bonds of 2.62 and 2.63 Å and one longer of 2.71 Å. Because of the adjoining vacancy site, the silver atoms surrounding the vacancy have lost coordination to one of their neighbors in the surface layer, which could lead to a stronger electronic interaction with the adsorbed Cl atom. In addition, the silver atoms bonded to the adsorbed chlorine atom can relax more extensively, and asymmetrically, to accommodate the Cl atom, which can thus approach the surface more closely. However, the effect is not large leading to the relatively small increase in adsorption energy.

Whereas we saw above that adsorption in the fcc site next to the vacancy was slightly more favourable than on the perfect surface, the opposite is true for adsorption at or near the adatom. When adsorbed to the adatom itself, the chlorine atom only forms one long Ag-Cl bond of 2.88 Å to the silver adatom, leading to the low adsorption energy of 113.4 kJ mol^{-1}. Again, the preferred position is in the fcc site next to the adatom (Fig. 5), where 136.3 kJ mol^{-1} is released, more favorable than at the adatom itself by almost 23 kJ mol^{-1}, which should ensure that the fcc site will be occupied preferentially over the adatom. However, adsorption in the fcc site next to the adatom is still hindered by the defect, leading to long Ag-Cl bonds of 2.73 Å to the two silver atoms surrounding the fcc site, which are furthest away from the adatom and 2.89 Å to the remaining silver atom, which is neighboring the adatom. This unfavourable interaction of the Cl atom with the surface silver atoms leads to the low adsorption energy of 136.3 kJ mol^{-1}, which compared to adsorption at the perfect surface (22 kJ mol^{-1} more favorable) should ensure that adsorption near surface adatoms will be less likely.

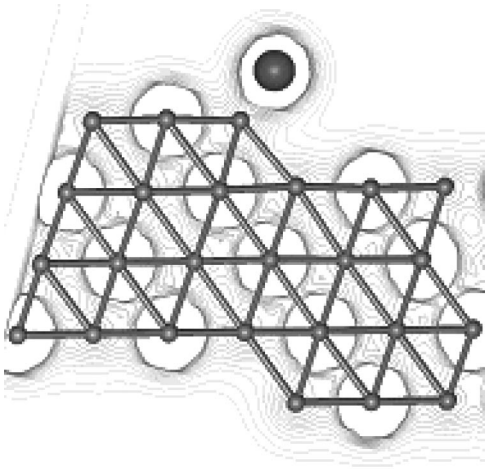

FIG. 6. Side view of the stepped (111) surface, with chlorine atom adsorbed at the step edge (electron density contour levels are from 0.02 to 0.30e/Å^3 at 0.02e/Å^3 intervals).

We next investigated chlorine adsorption at various sites near the step edge. However, all starting positions of the chlorine atom led to the same final configuration upon electronic and geometry optimization, where the chlorine atom becomes attached to two silver atoms on the step edge at 2.48 and 2.53 Å, without interactions to silver atoms on the terrace below the step, where the distance to the nearest silver atom is found to be 4.20 Å. Even when the chlorine atom was initially positioned on the terrace below the step, upon relaxation the chlorine atom moved away to the position shown in Fig. 6. The energy released upon adsorption at the step edge is 163.9 kJ mol^{-1} (Table II), which is larger than on the perfect surface, but only by 5.5 kJ mol^{-1}, which is not enough to direct Cl adsorption towards these edge sites to a significant extent.

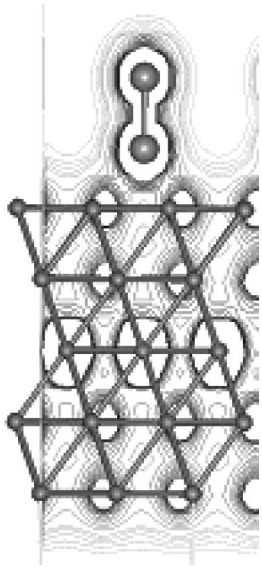

FIG. 7. Side view of the perfect (111) surface, with a chlorine molecule associatively chemisorbed to the fcc site, showing covalent Cl-Cl and partially covalent Ag-Cl bonding (electron density contour levels are from 0.02 to 0.30e/Å^3 at 0.02e/Å^3 intervals).

TABLE III. Energies of adsorption of molecular chlorine at the perfect (111) surface.

Adsorption energies of Cl_2 molecule at adsorption sites on the perfect (111) surface ($kJ\,mol^{-1}$)		
Associated		−42.8
Dissociated	Configuration 1	−230.6
	Configuration 2	−215.7
	Configuration 3	−217.1
	Configuration 4	−228.0

Adsorption of a Cl_2 molecule

We finally investigated the adsorption of a Cl_2 molecule at the silver (111) surface. As our calculations of adsorption of atomic chlorine described above have shown that the adsorption energies are not significantly enhanced by the presence of defects and that adsorption at defects is thus not particularly preferred and even hindered by the presence of adatoms, we have concentrated on adsorption of Cl_2 at the perfect (111) surface only. One of the initial configurations we investigated was a Cl_2 molecule adsorbed at the fcc site, but perpendicular to the surface. However, the Cl_2 molecule remained associated and only a lengthening of the Cl-Cl bond from 2.00 to 2.40 Å occurred upon electronic and geometry optimization, shown in Fig. 7. The electron density contour plots show that the Cl-Cl bond is purely covalent and that there is also some covalency in the Ag-Cl bonds, to the same extent as was found for adsorption of atomic chlorine on the planar surface. The Cl atom closest to the surface is located in the fcc site, in almost exactly the same position as atomic Cl adsorbed at this site, with only a marginally shorter Ag-Cl bond of 2.65 Å (instead of 2.66 Å). The adsorption energy, calculated according to equation (2), is very small, only 42.8 $kJ\,mol^{-1}$ (Table III) and as the adsorption of atomic chlorine is calculated to release well over 300 $kJ\,mol^{-1}$ for two dissociated chlorine atoms, this result suggests either that there may be a significant energy barrier to dissociation of the chlorine molecule and/or that the perpendicular configuration of the Cl_2 molecule on the surface is a local minimum energy position. However, experimentally, chlorine is found to adsorb in a dissociative fashion, indicating that there may not be a significant energy barrier to Cl_2 dissociation.[77] We therefore investigated a number of different starting configurations, where the Cl_2 molecule was initially positioned parallel to the surface in two directions and at a 45° angle to the surface, also pointing in two directions. These parallel and angled initial starting configurations all lead to dissociation of the Cl_2 molecule, indicating that the perpendicular position was indeed a local minimum, but they did not lead to the same final configurations, which gave us the opportunity to investigate the effect of the relative final positions of the two dissociated chlorine atoms on the adsorption energies, E_{ads}, which are given by:

$$E_{ads} = E_{slab+Cl_2} - [E_{slab} + E(Cl_2)]. \quad (2)$$

In the lowest energy final configuration, one chlorine atom of the dissociated Cl_2 molecule is adsorbed in a fcc site on the (111) surface (labeled 1) with the other atom adsorbed in a hcp site (labeled 2). As a result, the 0.5 monolayer coverage of adsorbed chlorine atoms forms a hexagonal honeycomb overlayer, which is rotated by approximately 35° with respect to the underlying 2×2 silver surface shown in Fig. 8(a), where each Cl-Cl distance is 3.40 Å. The Cl atoms in the fcc sites are bonded to two Ag atoms at a distance of 2.58 Å and to the third Ag atom at a distance of 2.69 Å. The Cl

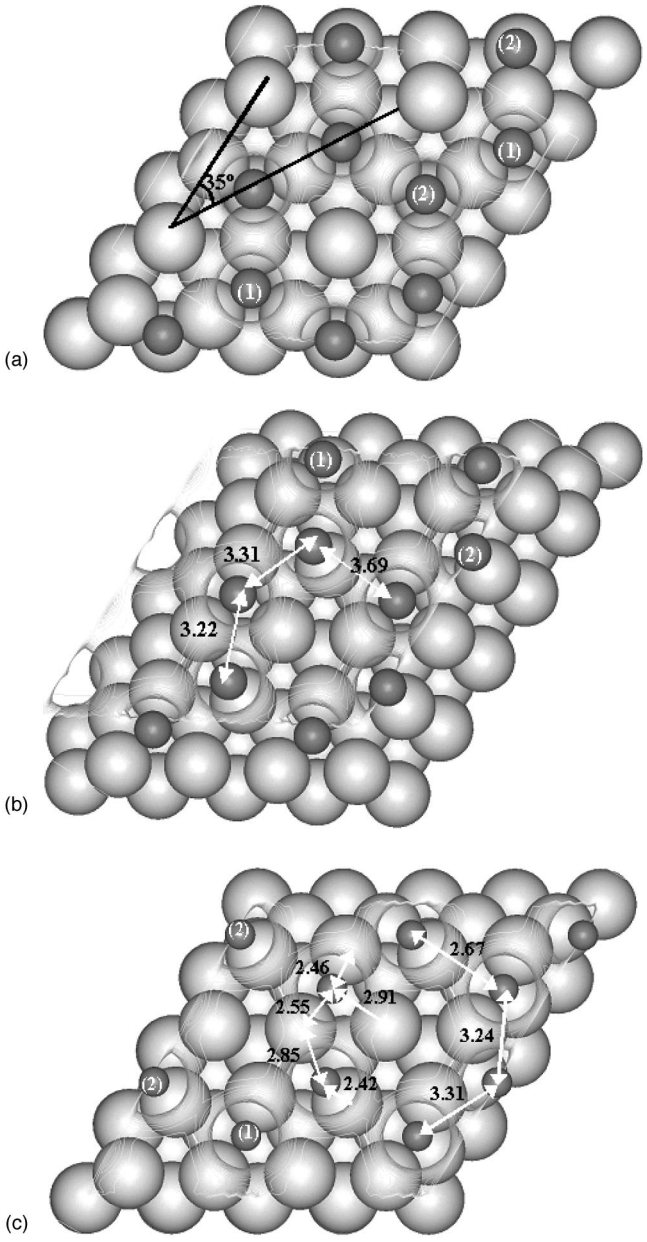

FIG. 8. Top views of (a) the lowest energy configuration 1 of the planar (111) surface with dissociatively adsorbed Cl_2 molecules in a hexagonal honeycomb structure, where Cl atom (1) is adsorbed in a fcc site and Cl atom (2) in a hcp site, with partially covalent bonding between the adsorbed Cl atoms; (b) the energetically least preferred chlorine overlayer, configuration 2, showing distortion of the hexagonal network; and (c) configuration 3, with Cl atoms (1) off-center from the fcc sites (distances in Å, electron density contour levels from 0.02 to 0.30e/$Å^3$ at 0.02e/$Å^3$ intervals).

atoms adsorbed in the hcp sites are bonded to two Ag atoms at 2.66 Å each and to the third at 2.56 Å. The Cl-Cl distance of 3.40 Å is less than double the van der Waals radius of chlorine (3.60 Å) and we may thus expect that some bonding interactions between the adsorbed chlorine atoms have been retained. Indeed, the electron density contour plots through the plane of the chlorine atoms show that some electron density is still distributed along the Cl---Cl axes (up to $0.06e\text{Å}^{-3}$) and the whole honeycomb overlayer thus forms a network of partially covalent interactions between the chlorine atoms.

The geometries and electronic distribution of the other chlorine overlayers are not as regular as the lowest energy configuration shown in Fig. 8(a). In the least favourable configuration shown in Fig. 8(b), which is however only $15\ \text{kJ mol}^{-1}$ less exothermic than Fig. 8(a), the chlorine atoms are still adsorbed in a honeycomb structure. However, even though half of the chlorine atoms are still adsorbed in fcc sites [labeled (1) in Fig. 8(b)], they are adsorbed off-center with one short Ag-Cl bond of 2.47 Å, one intermediate bond at 2.60 Å, and one long interaction at 2.81 Å. The other half of the chlorine atoms, labeled 2, have become adsorbed in a semi-bridging position, bonded to only two silver atoms at 2.41 and 2.86 Å. We see from Fig. 8(b) that, although the electron density is still to some extent spread out over the hexagonal network of chlorine atoms, the distribution is far less uniform than in Fig. 8(a) and the Cl-Cl distances also vary between 3.22 and 3.69 Å. The chlorine overlayer actually more closely resembles parallel ''zigzag'' lines on the surface, with alternating Cl-Cl distances of 3.22 and 3.31 Å and considerable overlap of electron density along the Cl---Cl axis. These ''zigzag'' lines interact with each other at certain points where the chlorine atoms are 3.69 Å apart, but with negligible electron density distributed along the axis between these chlorine atoms. Configuration 3, shown in Fig. 8(c), is intermediate between Figs. 8(a) and 8(b), both in terms of energy released upon adsorption of Cl_2 (Table III) and in terms of final configuration of the adsorbed chlorine atoms at the surface. This configuration has virtually the same energy of adsorption of Cl_2 ($-217.1\ \text{kJ mol}^{-1}$) as configuration 2 in Fig. 8(b) ($-215.7\ \text{kJ mol}^{-1}$), and the structure of the chlorine overlayer is similar. The chlorine atoms that are adsorbed off-center in the fcc site, labeled 1 in Fig. 8(c), are coordinated to the three surrounding surface silver atoms at Ag-Cl distances of 2.46, 2.55, and 2.91 Å, whereas the other chlorine atoms are adsorbed midway between a bridging and atop position, coordinated to two silver atoms at 2.42 and 2.85 Å.

The fourth structure, shown in Fig. 9, however, is different from the previous three in that the chlorine overlayer is buckled with respect to the surface, i.e., the hexagonal honeycomb structure which is flat with respect to the surface in configurations 1–3 is no longer so in configuration 4, as shown in Fig. 9(a). Its adsorption energy of $228.0\ \text{kJ mol}^{-1}$ is close to that of the energetically preferred configuration in Fig. 8(a) and the chlorine overlayer is stabilized by strong interactions with the surface silver atoms. The chlorine atoms which are farthest away from the surface, labeled 1 in Fig. 9, form single bonds to one surface silver atom each,

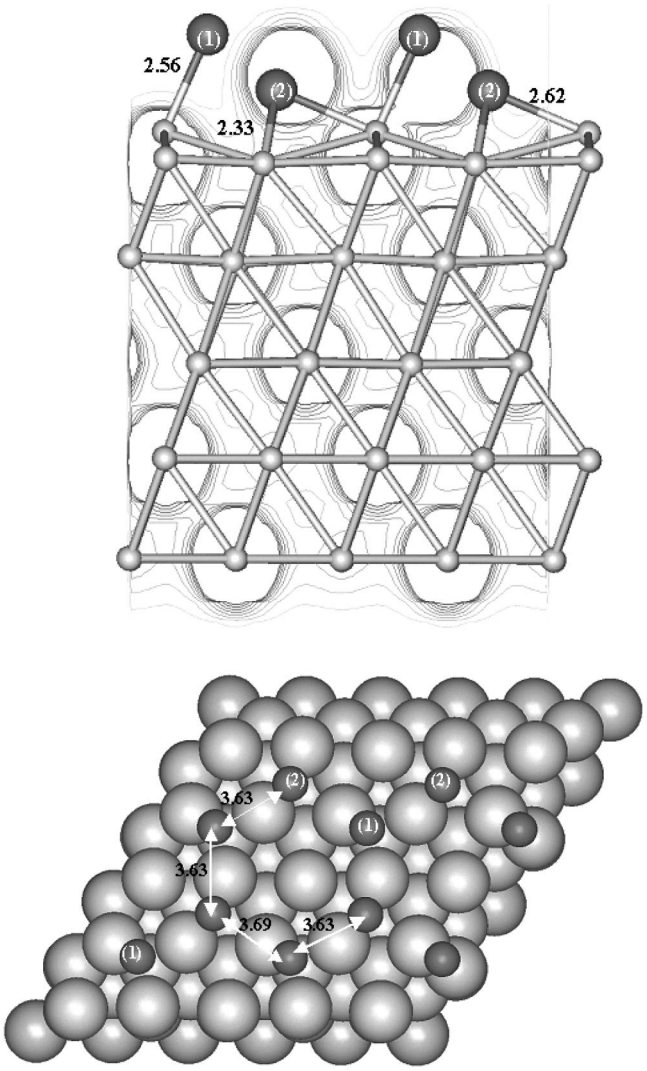

FIG. 9. (a) Side view of the nonplanar chlorine overlayer on the silver (111) surface, showing the flat electronic structure of the overlayer. (b) Plan view, showing Cl-Cl distances (distances in Å, electron density contour plots through the plane of both types of chlorine atoms and the top silver layer, from 0.05 to $0.40e/\text{Å}^3$ at $0.05e/\text{Å}^3$ intervals).

with a large degree of covalent bonding. Up to $0.43e\text{Å}^{-3}$ is distributed along the 2.56 Å long Ag-Cl bond, compared to $0.20e\text{Å}^{-3}$ for the Cl atom in the fcc site in the $\sqrt{3} \times \sqrt{3}R30^0$ chlorine overlayer described above. The other chlorine atoms (type 2), which are adsorbed closer to the surface, form two very short bonds of 2.33 Å to surface silver atoms, with a similar degree of covalency (up to $0.40e\text{Å}^{-3}$). The type 2 chlorine atoms are further coordinated to a third silver atom at 2.62 Å, which is the same as is bonded to the type 1 chlorine atom. As a result of these interactions with both types of chlorine atoms, the silver atom is pulled out of the surface plane by approximately 0.7 Å [Fig. 9(a)]. However, although the two types of chlorine atoms are at different heights above the silver plane ($\Delta r = 1.3$ Å), we see from Fig. 9(a), which shows electron density contour plots through both types 1 and 2 chlorine atoms (and the silver layers), that the electron density for both chlo-

rines is located at the same height above the surface, offset out of the plane from the geometrical position of Cl(1) and into the surface from the geometrical position of Cl(2). Thus, even though the atomic geometry of the chlorine overlayer is buckled, the electronic structure is flat, similar to configurations 1–3. The Cl-Cl distances are fairly regular at 3.63 Å in a zigzag pattern similar to Fig. 8(b) and at 3.69 Å between the rows, shown in Fig. 9(b).

DISCUSSION

Our results of adsorption of chlorine atoms at the fcc, hcp, bridge and top sites of the perfect (111) surface agree with those of Doll and Harrison,[49] who used the simulation code CRYSTAL, which employs a local basis set formalism where the basis functions are Gaussian type orbitals centered at the atoms, to calculate adsorption energies at the same four adsorption sites. They also found the preference for adsorption of fcc>hcp>bridge>atop for chlorine adsorption at one side only in $\sqrt{3}\times\sqrt{3}$ simulation cells of three and four layers thickness, with the fcc and hcp sites equally amenable to adsorption to within about 1 $kJ\,mol^{-1}$ and a difference of about 7 $kJ\,mol^{-1}$ between the hcp and bridge sites. Their calculated dissociative adsorption energy per Cl_2 molecule of -323 $kJ\,mol^{-1}$ agrees well with ours of -314 $kJ\,mol^{-1}$ for adsorption at the fcc site, whereas a different computational study of chlorine adsorption at the fcc site of a small cluster of silver atoms representing the (111) surface, showed calculated adsorption energies of between -309 and -386 $kJ\,mol^{-1}$ depending on the cluster,[83] although it is not clear from this paper whether these energies are calculated with respect to a Cl atom or a Cl_2 molecule.

Experimental studies of Cl_2 adsorption at the silver (111) surface showed chemisorption of atomic chlorine measuring adsorption energies of 209 to 231 $kJ\,mol^{-1}$ per Cl_2 molecule.[77,84] Our calculated adsorption energies of adsorption of Cl_2 range from 216 to 231 $kJ\,mol^{-1}$, which are clearly in excellent agreement with these experimentally found adsorption energies.[77,84] However, Goddard and Lambert[77] argued that their adsorption energy of 209 $kJ\,mol^{-1}$, which was based on an assumed preexponential factor in the interpretation of their data, was too low as the complete absence of Cl_2 desorption indicates that the chlorine has adsorbed in a dissociative fashion, which entails breaking the Cl-Cl chemical bond with an experimental dissociation energy of 239 $kJ\,mol^{-1}$ and hence dissociative adsorption of Cl_2 should release enough energy to overcome the dissociation energy of the Cl_2 molecule. Their view that an adsorption energy of 209 $kJ\,mol^{-1}$ is not enough for dissociative adsorption of Cl_2 would agree with our calculations of the adsorption of atomic chlorine, if we assume that the adsorption energy of Cl_2 is just twice that of an atomic chlorine atom (i.e., about two times 155–160 $kJ\,mol^{-1}$). However, our calculations of the adsorption of a Cl_2 molecule, rather than atomic chlorine, show that at a coverage of 0.5, which is the same as that found by Goddard and Lambert on the silver (111) surface,[77] the chlorine atoms do not become completely dissociated and isolated from each other, but form instead a regular network of chlorine atoms, kept together by partially covalent interactions. Because the interactions between the chlorine atoms is weak and they are not adsorbed in a pair-wise fashion, subsequent desorption is more likely to occur as atomic chlorine than as Cl_2 molecules, as is observed experimentally.[77,84] For example, when we calculate the energy of the energetically preferred chlorine overlayer [Fig. 8(a)] without the underlying silver surface, the residual energy (i.e., the energy of the chlorine overlayer with respect to isolated chlorine atoms) is -58.4 $kJ\,mol^{-1}$ per chlorine atom. This energy is, however, an upper value as it is based on a electronic relaxation without geometry optimization of the chlorine overlayer only, and as such it does not take into account the electronic interactions with the silver atoms in the surface, which will lower the interchlorine interaction. However, this calculation shows that in the extreme case, another 58.4 $kJ\,mol^{-1}$ per chlorine atom, i.e., about 117 $kJ\,mol^{-1}$ per adsorbed Cl_2 molecule, should have to be expended if the chlorine network were to be fully dissociated into isolated chlorine atoms. Despite the apparent anomaly between the experimental adsorption energies and the desorption of atomic chlorine off the surface, the experimentally measured adsorption energies of up to 231 $kJ\,mol^{-1}$, which are confirmed by our calculated energies of Cl_2 adsorption, are compatible with an extended network of partially dissociated Cl_2 molecules, which are stabilized by residual covalent interchlorine interactions. In addition, the higher coverage of chlorine atoms could lead to repulsive lateral interactions between the chlorine atoms or a decrease of the Ag-Cl bond strength due to some of the Cl atoms sharing particular silver atoms, all of which would lead to a smaller adsorption energy of the dissociated Cl_2 molecules compared to atomic chlorine.

Another issue of debate has been the Ag-Cl bond length, once chlorine was adsorbed at the silver (111) surface, and the chlorine overlayer structure. At low coverages of approximately 1/3 monolayer there are strong experimental indications that a $\sqrt{3}\times\sqrt{3}R30^0$ pattern of chlorine atoms is favored,[76–78] followed by higher density structures at increased coverages up to saturation, although the reported coverages vary widely.[76–78,85–88] Schott and White use scanning tunneling microscopy on atomically flat silver (111) terraces, where at a coverage of 0.6 they identify a chlorine overlayer as a double row configuration on the surface, separated by transition regions of hexagonal patterns. This configuration of the overlayer is similar to our structure in Fig. 8(b), but with one extra chlorine atom in the middle of each distorted chlorine hexagon. In surface regions with coverages of approximately 0.45 they observe incomplete chlorine adlayers, which are identical to our honeycomb structures. The agreement is especially good with our configuration 2 shown in Fig. 8(b), where the chlorine atoms are adsorbed at both fcc and semibridge sites. Schott and White observe chlorine rows of different brightness, indicating two types of adsorption sites for the chlorine atoms, which are consistent with threefold hollow and twofold bridge sites. They measured Cl-Cl distances of 3.8 and 3.3 Å, which agree very well with our calculated Cl-Cl distances of 3.69 and 3.22 Å in Fig. 8(b). Lamble *et al.*[85] used low energy electron diffrac-

tion (LEED) and surface extended x-ray absorption fine-structure (SEXAFS) measurements to identify an alternative vacancy honeycomb structure at a coverage of 0.67, which is of course a more densely packed structure than our chlorine overlayers, but other workers tend to disagree with their reported coverage. Schott and White argued that Lamble *et al.*'s SEXAFS data should be reinterpreted, as LEED will have given an average structure of the three different STM patterns identified by Schott and White. If the SEXAFS data take into account this averaging of the structures, the LEED/SEXAFS results are consistent with the STM results of Schott and White. Our calculations of the 0.5 monolayer coverages clearly show that it is possible to obtain a range of different chlorine overlayers, which are energetically similar. As such, it is quite feasible that Lamble *et al.* obtained different adsorption patterns, giving average data.

Lamble *et al.* measure an Ag-Cl bond length of 2.70 Å,[85] whereas Shard and Dhanak, also using SEXAFS, measure Ag-Cl bondlengths of only 2.48 Å.[78] Previous calculations, based only on adsorption of atomic chlorine in the $\sqrt{3} \times \sqrt{3}R30^0$ configuration were unable to resolve the matter as the calculated Ag-Cl bondlengths were intermediate at 2.62 or 2.55 Å, depending on the approximations used in the DFT techniques.[49] However, based on our calculations, we conclude that both can be correct depending on the adsorption site and configuration of the adsorbed chlorine atoms. Firstly, we found in our simulations of atomic chlorine at different surface features, that surface defects have a distinct effect on the Ag-Cl bond lengths, which were calculated to range from 2.48 and 2.53 Å at the step edge, through 2.66 Å on the perfect surface, to 2.62 and 2.71 Å at the vacancy site and 2.73 Å at the adatom site. Several experimental studies have found that at high chlorine dosages, layers of silver chloride are formed at the silver (111) surface.[87–91] For example, the STM studies of silver (111) chlorination by Andryushechkin *et al.* showed that AgCl islands usually nucleate at surface defects such as atomic steps,[90] and more rarely on the terraces.[91] Certainly, the short Ag-Cl bond lengths for the chlorine atoms adsorbed at the step edges suggest the formation of a phase, which is closer to silver chloride than are the chemisorbed chlorine molecules on the planar surface. We saw that the chlorine atoms ''preferred'' to adsorb to the step edge, coordinating to only two silver atoms, rather than in the fcc site on the terrace below, where they would be coordinated to three silver atoms but at longer Ag-Cl distances. However, when chlorine is adsorbed at the step edge the Ag-Cl-Ag angle is 72°, which although slightly larger than in the fcc site (68.8°) is still not very close to the silver chloride structure (90°). Clearly, the stronger interaction with two silver atoms outweighs the higher coordination number of the fcc site, but although the resultant AgCl structure is slightly closer to crystalline silver chloride than the chlorine adatoms at the planar surface, it would need a great many further calculations to elucidate the process of formation of a silver chloride phase at the step edges.

In addition to the variation in Ag-Cl bond distances at the surface defects discussed above, even considering only the perfect planar (111) surface, which is similar to the atomically flat terraces studied experimentally, we found that adsorption of Cl_2 molecules in a bigger simulation cell led to four structurally different, but energetically almost identical, chlorine overlayers. When adsorbed in the lowest energy configuration [Fig. 8(a)], all chlorine atoms are located in three-fold hollow sites (fcc and hcp) and the Ag-Cl bondlengths range from 2.56 to 2.69 Å, i.e., close to the value of 2.70 ± 0.02 measured by Lamble *et al.*[85] However, in the energetically least preferred configuration [Fig. 8(b)], the distortion of the honeycomb structure and adsorption of chlorine atoms off-center in the fcc sites and away from the hcp site onto a semibridge site, leads to a significant shortening of some of the Ag-Cl bonds to 2.41 and 2.47 Å, i.e., close to the value found by Shard and Dhanak, even though their overlayer is only 1/3 of a monolayer and hence not directly comparable with our 0.5-ML structures.[78] However, our findings show that at a particular coverage, it is perfectly feasible to obtain structurally very different adsorption layers which are energetically very similar. The structure of configuration 4, shown in Fig. 9, which is energetically comparable to the lowest energy configuration, is even more extreme than the previous configurations in that some of the Ag-Cl bond lengths have shortened to 2.33 Å, i.e., even closer to the Ag-Cl bonds in the silver chloride structure (2.28 Å) than at the step edges. This latter result confirms LEED and thermal desorption experiments by Bowker and Waugh, who identified an AgCl layer on the silver (111) surface, which desorbed from the surface as AgCl molecules,[87] x-ray photoemission spectroscopy data by Kawasaki and Ishii, identifying the formation of an epitaxial silver chloride layer on a thin silver (111) film[89] and the formation of silver chloride islands on the planar terraces observed by STM measurements by Andryushechkin *et al.*[91]

CONCLUSION

We have executed a series of electronic structure calculations, based on density functional theory, of the adsorption of chlorine at the ideal and three defective (111) surfaces of silver. We find that on the planar surface, chlorine atoms show an energetic preference for adsorption in the hollow sites, with virtually equal adsorption energies for the fcc and hcp sites. Adsorption at or near surface defects has only a marginal effect on the adsorption energy, apart from adsorption near the adatom, which is energetically less favourable by 22 kJ mol^{-1}. As the gain in energy of chlorine adsorption at the step or vacancy in the surface is at most 8 kJ mol^{-1} for adsorption in the fcc site next to a silver vacancy, we expect no significant preferential adsorption at the defect sites in view of the almost equally large adsorption energies at the normal sites on the perfect (111) surface. Apart from adsorption at the step on the (111) surface, where the chlorine atom becomes attached to two silver atoms on the step edge, adsorption at the other surface defects, vacancies and adatoms, is preferred in the fcc sites next to the defect rather than in the vacancy or on the adatom itself.

In addition, we have studied the adsorption of chlorine molecules at the planar (111) surface at a coverage of 0.5, where we found a series of energetically similar chlorine

overlayers. The differences in energies between these four stable structures were small enough that there would be no significant energetic driving force for a transition of one configuration into a lower energy structure. Most configurations were based on a planar hexagonal honeycomb structure, with chlorine atoms adsorbed in stable hollow and semibridge sites on the surface, which agreed well with experimentally found overlayer structures,[86] although in our calculations the 0.5 monolayer structures were confined to 2×2 surface supercells and it is quite possible that alternative structures would be obtained as well, if we were to consider different supercells. The chlorine molecules were almost completely dissociated, but were not only held together in the overlayer structure through interactions to the surface, but also by a network of covalent interactions between the chlorine atoms themselves, which could explain why Goddard and Lambert found an adsorption energy which was lower than the full dissociation energy of Cl_2, in good agreement with our calculated energies for Cl_2 adsorption.[77] One of the energetically most favourable overlayers has the chlorine atoms adsorbed at different heights above the surface, although the electronic structure of the overlayer is planar. The silver-chlorine bondlength in this case suggests the formation of a silver chloride structure, in agreement with experiment where desorption of AgCl molecules was found to occur.[87]

Even without taking into account surface defects, the overlayer structures from dissociated Cl_2 molecules,[92] which are all energetically similar, exhibit a large range of calculated silver-chlorine bondlengths, from 2.33 Å for the nonplanar structure, through 2.47 Å for a planar but irregular structure, to 2.69 Å for the regular lowest energy overlayer. Hence, the experimentally measured bondlengths of 2.48 and 2.70 Å plus the silver chloride layer, rather than being mutually exclusive are all equally likely, depending on the particular overlayer structure formed in the experiment. As they are energetically calculated to be within 15 kJ mol^{-1} of one another, the formation of one particular structure over another may well be due to experimental set up and kinetic factors rather than on thermodynamic grounds. Our study has hence shown that adsorption of chlorine on the silver (111) surface can lead to a range of energetically similar but structurally very dissimilar chlorine overlayers, which may explain the apparently conflicting evidence from experimental studies.

Future work will include further calculations of chlorine adsorption at higher coverages and in different configurations. In addition, we plan detailed calculations of the coadsorption of chlorine and ethene at the (111) surface to determine the effect of chlorine on the reactivity of the silver surface towards ethene, which is experimentally found to be strongly dependent upon chlorine coverage.[93,94]

ACKNOWLEDGMENTS

C.J.N. thanks Dr B. Slater for useful discussions, the EPSRC for a studentship and the European Union for a Marie Curie Fellowship. N.H.dL. thanks EPSRC for an Advanced Research Fellowship, the Royal Society Grant No. 22292 for funding and the EPSRC Materials Chemistry Consortium for provision of computational facilities on the Cray T3E and HPCx high performance computing systems.

*Email address: n.h.deleeuw@ucl.ac.uk

[1] J.G. Serafin, A.C. Liu, and S.R. Seyermonir, J. Mol. Catal. A **131**, 157 (1998).
[2] V.I. Bukhtiyaros, I.P. Prosvirin, R.I. Kvon, S.N. Goncharova, and B.S. Bal'zhinimaev, J. Chem. Soc., Faraday Trans. **93**, 2323 (1997).
[3] R. Koch, M. Sturmat, and J.J. Schulz, Surf. Sci. **454**, 543 (2000).
[4] S. Kagami, H. Minoda, and N. Yamamoto, Surf. Sci. **493**, 78 (2001).
[5] J. Bremer, J.-K. Hansen, K. Stahrenberg, and T. Worren, Surf. Sci. **459**, 39 (2000).
[6] B. Degroote, J. Dekoster, and G. Langouche, Surf. Sci. **452**, 172 (2000).
[7] B.A.F. Puygranier, P. Dawson, Y. Lacroute, and J.-P. Goudonnet, Surf. Sci. **490**, 85 (2001).
[8] Y. Oshima, H. Nakade, S. Shigeki, H. Hirayama, and K. Takayanagi, Surf. Sci. **493**, 366 (2001).
[9] B.D. Yu and M. Scheffler, Phys. Rev. Lett. **77**, 1095 (1996).
[10] R.C. Longo, C. Rey, and L.J. Gallego, Surf. Sci. **459**, L441 (2000).
[11] F. Baletto, C. Mottet, and R. Ferrando, Phys. Rev. Lett. **84**, 5544 (2000).
[12] S.J. Zhao, S.Q. Wang, Z.Q. Yang, and H.Q. Ye, J. Phys.: Condens. Matter **13**, 8061 (2001).
[13] F. Baletto and R. Ferrando, Surf. Sci. **490**, 361 (2001).
[14] S. Narasimhan, Surf. Sci. **496**, 331 (2002).
[15] T. Itoyama, M. Wilde, M. Matsumoto, T. Okano, and K. Fukutani, Surf. Sci. **493**, 84 (2001).
[16] X.-C. Guo and R.J. Madix, Surf. Sci. **496**, 39 (2002).
[17] X.-C. Guo and R.J. Madix, Surf. Sci. **489**, 37 (2001).
[18] M.E. Alikhani, J. Chem. Soc., Faraday Trans. **93**, 3305 (1997).
[19] A.J. Nagy, G. Mestl, T. Rühle, G. Weinberg, and R. Schögl, J. Catal. **179**, 548 (1998).
[20] J. Lee, S. Ryu, and S.K. Kim, Surf. Sci. **481**, 163 (2001).
[21] I. Lee, S.K. Kim, W. Zhao, and J.M. White, Surf. Sci. **499**, 41 (2002).
[22] G. Compagnini, A. De Bonis, R.S. Cataliotti, and G. Marletta, Phys. Chem. Chem. Phys. **2**, 5298 (2000).
[23] M. Zharnikov, S. Frey, H. Rong, Y.-J. Yang, K. Heister, M. Buck, and M. Grunze, Phys. Chem. Chem. Phys. **2**, 3359 (2000).
[24] H. Kondoh, H. Tsukabayashi, T. Yokoyama, and T. Ohta, Surf. Sci. **489**, 20 (2001).
[25] L.A. Peyser, T.H. Lee, and R.M. Dickson, J. Phys. Chem. B **106**, 7725 (2002).
[26] P.V. Kamat, J. Phys. Chem. B **106**, 7729 (2002).
[27] C.J. Bertole and C.A. Mims, J. Catal. **184**, 224 (1999).
[28] A.J. Nagy, G. Mestl, and R. Schögl, J. Catal. **188**, 56 (1999).
[29] C.I. Carlisle, D.A. King, M.L. Bocquet, J. Cerda, and P. Sautet, Phys. Rev. Lett. **84**, 3899 (2000).
[30] A.J. Nagy, G. Mestl, D. Herein, G. Weinberg, E. Kitzelmann, and R. Schlögl, J. Catal. **182**, 417 (1999).
[31] G.J. Millar, M.L. Nelson, and P.J.R. Uwins, J. Chem. Soc., Faraday Trans. **94**, 2015 (1998).
[32] W.-X. Li, C. Stampfl, and M. Scheffler, Phys. Rev. B **65**, 075407 (2002).

[33] Y. Wang, L.L. Jia, W.N. Wang, and K.N. Fan, J. Phys. Chem. B **106**, 3662 (2002).
[34] M.R. Salazar, J.D. Kress, and A. Redondo, Surf. Sci. **469**, 80 (2000).
[35] A. Michaelides, M.-L. Bocquet, P. Sautet, A. Alavi, and D.A. King, Chem. Phys. Lett. **367**, 344 (2003).
[36] M.-L. Bocquet, A. Michaelides, P. Sautet, and D. King, Phys. Rev. B **68**, 075413 (2003).
[37] D. Stacchiola, G. Wu, M. Kaltchev, and W.T. Tysoe, Surf. Sci. **486**, 9 (2001).
[38] V.I. Avdeev and G.M. Zhidomirov, Surf. Sci. **492**, 137 (2001).
[39] Q. Sun, Y. Wang, K. Fan, and J. Deng, Surf. Sci. **459**, 213 (2000).
[40] M.-L. Bocquet, P. Sautet, J. Cerda, C.I. Carlisle, M.J. Webb, and D.A. King, J. Am. Chem. Soc. **125**, 3119 (2003).
[41] M.-L. Bocquet, A. Michaelides, D. Loffreda, P. Sautet, A. Alavi, and D. King, J. Am. Chem. Soc. **125**, 5620 (2003).
[42] S. Hawker, C. Mukoid, J.P.S. Badyal, and R.M. Lambert, Surf. Sci. **219**, L615 (1989).
[43] E.R. Frank and R.J. Hamers, J. Catal. **172**, 406 (1997).
[44] G. Wu, D. Stacchiola, M. Kaltchev, and W.T. Tysoe, Surf. Sci. **463**, 81 (2000).
[45] P. Hollins, A.A. Davis, D.A. Slater, M.A. Chesters, E.C. Hargreaves, P.M. Parlett, J.C. Wenger, and M. Surman, J. Chem. Soc., Faraday Trans. **92**, 879 (1996).
[46] O. Endo, H. Kondoh, Y. Yonamoto, E.M. Staicu-Casagrande, S. Lacombe, L. Guillemot, V.A. Esaulov, L. Pasquali, S. Nannarone, and M. Canepa, Surf. Sci. **480**, L411 (2001).
[47] B. Shen, Z. Fang, K. Fan, and J. Deng, Surf. Sci. **459**, 206 (2000).
[48] Y. Wang, W. Wang, K. Fan, and J. Deng, Surf. Sci. **487**, 77 (2001).
[49] K. Doll, and N.M. Harrison, Phys. Rev. B **63**, 165410 (2001).
[50] G. Kresse and J. Hafner, Phys. Rev. B **47**, 558 (1993).
[51] G. Kresse and J. Hafner, Phys. Rev. B **49**, 14 251 (1994).
[52] G. Kresse and J. Furthmüller, J. Comput. Mater. Sci. **6**, 15 (1996).
[53] G. Kresse and J. Furthmüller, Phys. Rev. B **54**, 11 169 (1996).
[54] R. Jones and O. Gunnarsson, Rev. Mod. Phys. **61**, 689 (1989).
[55] M. Payne, M. Teter, D. Allan, T. Arias, and J. Joannopoulos, Rev. Mod. Phys. **64**, 1045 (1992).
[56] M. Gillan, Contemp. Phys. **38**, 115 (1997).
[57] N.T. Barrett, C. Guillot, B. Villette, G. Treglia, and B. Legrand, Surf. Sci. **251**, 717 (1991).
[58] J.E. Klepeis, L.J. Terminello, and D.A. Lapiano Smith, Phys. Rev. B **53**, 16 035 (1996).
[59] L. Stauffer, A. Mharchi, S. Saintenoy, C. Pirri, P. Wetzel, D. Bolmont, and G. Gewinner, Phys. Rev. B **52**, 11 932 (1995).
[60] D.M. Swanston, A.B. McLean, D.N. McIlroy, D. Heskett, R. Ludeke, H. Munekata, M. Prietsch, and N.J. DiNardo, Surf. Sci. **312**, 361 (1994).
[61] L.N. Kantorovich, J.M. Holender, and M.J. Gillan, Surf. Sci. **343**, 221 (1995).
[62] P.J.D. Lindan, J. Muscat, S. Bates, N.M. Harrison, and M. Gillan, Faraday Discuss. **106**, 135 (1997).
[63] P.J.D. Lindan, N.M. Harrison, and M.J. Gillan, Phys. Rev. Lett. **80**, 762 (1998).
[64] J.P. Perdew, J.A. Chevary, S.H. Vosko, K.A. Jackson, M.R. Pederson, D.J. Singh, and C. Fiolhas, Phys. Rev. B **46**, 6671 (1992).
[65] N.H. de Leeuw, and C.J. Nelson, J. Phys. Chem. B **107**, 3528 (2003).
[66] J. Goniakowski and M.J. Gillan, Surf. Sci. **350**, 145 (1996).
[67] N.H. de Leeuw, J.A. Purton, S.C. Parker, G.W. Watson, and G. Kresse, Surf. Sci. **452**, 9 (2000).
[68] D. Vanderbilt, Phys. Rev. B **41**, 7892 (1990).
[69] G. Kresse and J. Hafner, J. Phys.: Condens. Matter **6**, 8245 (1994).
[70] H.J. Monkhorst and J.D. Pack, Phys. Rev. B **13**, 5188 (1976).
[71] M. Methfessel and A.T. Paxton, Phys. Rev. B **40**, 3616 (1989).
[72] C. Kittel, *Introduction to Solid State Physics* (Wiley, New York, 1996).
[73] Y. Wang, W. Wang, K.-N. Fan, and J. Deng, Surf. Sci. **490**, 125 (2001).
[74] S.M. Foiles, M.I. Baskes, and M.S. Daw, Phys. Rev. B **33**, 7983 (1986).
[75] K. Refson, R.A. Wogelius, D.G. Fraser, M.C. Payne, M.H. Lee, and V. Milman, Phys. Rev. B **52**, 10 823 (1995).
[76] G. Rovida, and F. Pratesi, Surf. Sci. **51**, 270 (1975).
[77] P.J. Goddard and R.M. Lambert, Surf. Sci. **67**, 180 (1977).
[78] A.G. Shard and V.R. Dhanak, J. Phys. Chem. B **104**, 2743 (2000).
[79] Y. Takata, H. Sato, S. Yagi, T. Yokoyama, and T. Ohta, Surf. Sci. **265**, 111 (1992).
[80] V.R. Dhanak, A.G. Shard, S. D'Addato, and A. Santoni, Chem. Phys. Lett. **306**, 341 (1999).
[81] M.F. Kadodwala, A.A. Davis, G. Scragg, B.C.C. Cowie, M. Kerkar, D.P. Woodruff, and R.G. Jones, Surf. Sci. **324**, 122 (1995).
[82] N.H. de Leeuw, S.C. Parker, C.R.A. Catlow, and G.D. Price, Am. Mineral. **85**, 1143 (2000).
[83] B. Shen, Z. Fang, K. Fan, and J. Deng, Surf. Sci. **459**, 206 (2000).
[84] Y.-Y. Tu and J.M. Blakeley, Surf. Sci. **85**, 276 (1979).
[85] G.M. Lamble, R.S. Brooks, S. Ferrer, D.A. King, and D. Norman, Phys. Rev. B **34**, 2975 (1986).
[86] J.H. Schott and H.S. White, J. Phys. Chem. **98**, 291 (1994).
[87] M. Bowker and K.C. Waugh, Surf. Sci. **134**, 639 (1983).
[88] B.V. Andryushechkin, K.N. Eltsov, V.M. Shevlyuga, and V.Y. Yurov, Surf. Sci. **407**, L633 (1998).
[89] M. Kawasaki and H. Ishii, Langmuir **11**, 832 (1995).
[90] B.V. Andryushechkin, K.N. Eltsov, V.M. Shevlyuga, and V.Y. Yurov, Surf. Sci. **431**, 96 (1999).
[91] B.V. Andryushechkin, K.N. Eltsov, and V.M. Shevlyuga, Surf. Sci. **433**, 109 (1999).
[92] Structural details and coordinates of the relaxed silver surfaces with chlorine overlayers are available from the corresponding author (n.h.deleeuw@ucl.ac.uk).
[93] D.A. Slater, P. Hollins, and M.A. Chesters, J. Electron Spectrosc. Relat. Phenom. **64**, 95 (1993).
[94] D.A. Slater, P. Hollins, and M.A. Chesters, Surf. Sci. **306**, 155 (1994).